annals of
NUCLEAR ENERGY

PERGAMON

Annals of Nuclear Energy 26 (1999) 709–728

The design and experimental validation of an emergency core cooling system for a pool type research reactor

Walmir Maximo Torres*, Benedito Dias Baptista Filho, Daniel Kao Sun Ting

Instituto de Pesquisas Energéticas e Nucleares, Travessa R, 400, Cidade Universitária, CEP 05598-900 São Paulo, SP, Brazil

Received 14 August 1998; accepted 21 September 1998

Abstract

This paper presents the design of the Emergency Core Cooling System (ECCS) for the IEA-R1m pool type research reactor. This system with passive features, uses sprays installed above the core. The experimental program performed to define system parameters and to demonstrate to the licensing authorities, that the fuel elements limiting temperature is not exceeded, is also presented. Flow distribution experiments using a core mock-up in full-scale were performed to define the spray header geometry and spray nozzles specifications as well as the system total flow rate. Another set of experiments using electrically heated plates simulating heat fluxes corresponding to the decay heat curve after full power operation at 5 MW was conducted to measure the temperature distribution at the most critical position. The observed water flow pattern through the plates has a very peculiar behavior resulting in a temperature distribution which was modelled by a 2D energy equation numerical solution. In all tested conditions the measured temperatures were shown to be below the limiting value.

1. Introduction

The IEA-R1m pool type research reactor using MTR fuel elements was designed by Babcok and Wilcox and since its first criticality in 1957 it has been operated at 2 MW power level, although its nominal design power is 5 MW. The IEA-R1m

*Corresponding author. Tel.: 00-55-011-816-9199; fax: 00-55-011-816-9432; e-mail: wmtorres@net.ipen.br.

PII: S0306-4549(98)00084-X

reactor is used for several basic researches, training, industrial applications and mainly for radioisotope production for medical use. In order to increase its production capability, a backfitting and upgrading program was designed and implemented during 1996/97 and after successfully completing the design, constructions and licensing, the reactor is running nowdays at full 5 MW.

According to Williams et al. (1969)Gehre et al. (1989), several research reactors around the world have undergone backfitting and upgrading programs with power increase and for that their safety conditions were reassessed either because new regulatory requirements were introduced or by new technological developments. Particularly, the loss of coolant accident with the need of removing the residual decay heat has merited special attention. Webster (1967), based on experimental data concluded that pool type research reactors using MTR type fuel elements operating with power levels up to 3 MW do not require emergency cooling since the maximum radioactive decay heat flux can be dissipated by natural convection air cooling without reaching unsafe temperatures. However, for powers above 3 MW, additional safety measures are necessary to assure core integrity under loss of coolant accident condition. Water spray cooling systems installed above the core are among the most commonly used.

To design such a system, the following basic design parameters are necessary: (a) the system total flow rate required to effectively remove the residual heat by using sprays; (b) spray flow rate distribution in the core in order to assure that every fuel element including the control fuel element are adequately cooled; (c) the minimum operational time required to remove the residual decay heat during the initial period of the loss of coolant accident until the heat flux is low enough that the core can be cooled by natural air convection. This last data together with the total system flow rate are used for dimensioning the storage tanks capacity. The above parameters were determined or verified experimentally.

This work is divided into six sections, Section 1 being the introduction. In Section 2, a description of the (ECCS) designed and installed in the IEA-R1m research reactor is presented with its main characteristics and a flow diagram. Section 3 presents the basic data base used for the design parameters definition such as decay power curves and heat flux distributions. In Section 4, the design validation experimental program to determine spray flow distribution and temperature distributions is described and the results are shown and discussed. The numerical model developed to describe the peculiar temperature behavior on the heated plates and to calculate the temperature difference between the experimental plates using a Ni–Cr alloy material as heated elements and the actual fuel material is included in Section 5. Finally, in Section 6, the most important conclusions are discussed.

2. Emergency core cooling system description

The emergency core cooling is done by regular tap water spraying. The water is stored in two independent elevated reservoirs that feed by gravity a spray header in U shape with spray nozzles located above the core.

The IEA-R1m ECCS flow diagram is shown in Fig. 1. It has two reservoirs with 75 m^3 capacity each, feeding two independent branches (A and B) linked to the spray header. Each reservoir when totally full and without water make-up, allows the system to operate at full design flow rate of 3.5 m^3/h for more than 20 h. This spraying flow rate is enough to keep the fuel plates temperature at a safe level as it will be demonstrated by the results with the heated plates experiments. Water level switches are installed in the reservoirs and alarm when a minimum level is reached. Below this minimum level the reactor is not allowed to operate at 5 MW. This minimum water level still guarantees 14 h of the ECCS operation.

The system is automatically actuated by low water level instruments located in the pool which signals solenoid valves to open when the level is abnormally low. The water level in the pool is monitored by independent level instruments with electrical power supplied by a no-break system. These solenoid valves can also be manually actuated through the control panel located in the Emergency Room away from potentially hazardous doses. The B branch can also be opened by the operators by actuaction of a manual fast action ball type valve which is located in the Emergency Room. The opening of any one of the valves is sufficient to assure that the design total flow rate is achieved.

The spray header, located 525 mm above the top of the fuel elements, is made of 2 in. diameter aluminum tubes in U shapped format. The header is fitted with seven spray nozzles which quantity, position, type and instalation angle were defined based on the flow distribution experiments described below. The connections

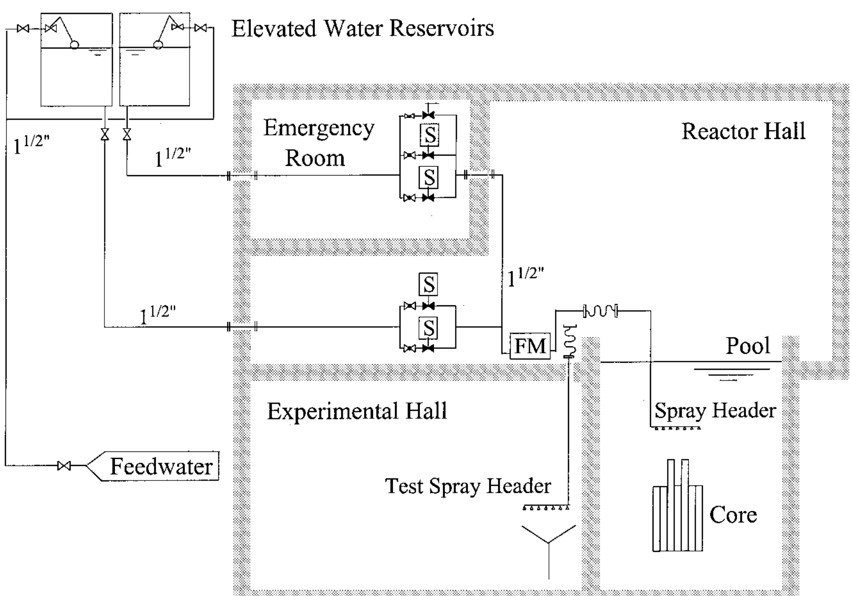

Fig. 1. IEA-R1m reactor emergency core cooling system diagram.

between the header and the feedwater line is done using flexible pipes and fast action connectors.

In order to perform periodical system testing, another header, with same characteristics, was constructed and installed in the basement which mocks-up the system and allows for weekly functional tests of the system before each start-up.

3. System design parameters

A 5 MW pool type research reactor with a 5×5 fuel elements core with 21 MTR type fuel element with 18 plates each and four control elements with 12 plates each, after infinite operation time has the decay heat power curve shown in Fig. 2. This decay power was calculated using ORIGEN code (Croff, 1980) and includes a 20% overestimation to account for safety margin. Under this condition, conservative calculations performed by Maprelian (1997) indicates that after approximately 13.5 h from the reactor shutdown, the natural circulation air cooling of the core is enough to assure that the fuel will not exceed 500°C in any part of the core in the case of complete loss of water. During this time period, emergency water must be supplied to cool the core and this time was used to calculate the minimum storage volume.

Burn (1997) calculated that the highest temperature in the core is expected to be around 310°C between 12.8 and 15.6 h after shutdown, using conservative modelling hyphothesis and cooling by natural air circulation. Additional tests besides the experiments described in this paper will be performed under natural air circulation

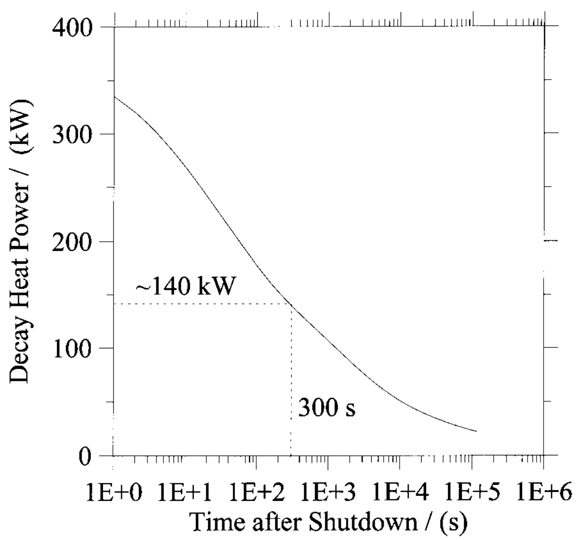

Fig. 2. Decay heat curve for 5MW IEA-R1m reactor.

cooling and heat flux corresponding to decay energy after 13.5 h to confirm this condition.

For the core configuration considered, the normalized axial power density distribution was calculated using LEOPARD code modified by Kerr et al. (1991) to model plate type fuel elements and CITATION (Flowler et al., 1971). Fig. 3 shows the axial core average power density and also the hot channel axial power density distribution. A 10% uncertainty factor is added to the above results. Assuming that these distributions are maintained during the decay period shown in Fig. 2, these curves were used to design the system and to define the experimental parameters.

The time to initiate the core uncovering after a full loss of collant accident in the reactor pool, calculated by Maprelian (1997), is approximately 300 s when the maximum heat flux in the hot channel is 1.13 W/cm^2. These values are considered as the initial conditions for the experiments.

Parkanski (1992) performed tests using uniformly heated plates and measured the maximum temperatures for various heat fluxes and under different cooling conditions resulting in the curves shown in Fig. 4. One can observe from these curves that for spray flow rates between 30 and 45 cm^3/min/plate it is possible to cool partially submerged fuel plates subjected to heat fluxes up to 4.5 W/cm^2 keeping the temperature under values around 110°C. These results were used for the development of the ECCS in the RP-10 peruvian reactor which has 10 MW and uses MTR type fuel, similar to the ones used by IEA-R1m reactor.

The IEA-R1m reactor ECCS spray flow rate was set at 3.5 m^3/h, constant over a minimum period of 13.5 h even considering that the power level is half of the RP-10

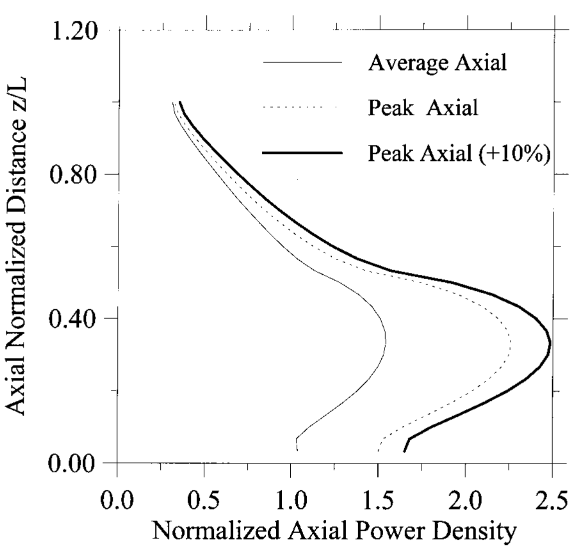

Fig. 3. Reactor normalized axial power profile.

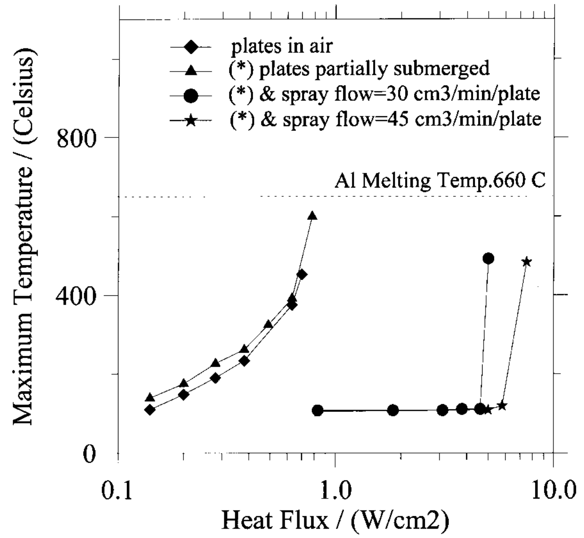

Fig. 4. Plates maximum temperature as function of the heat flux.

reactor. However, the accident considered for the IEA-R1m reactor is more severe since it assumes the total uncovering of the core while the RP-10 reactor considers partial uncovering at the beam ports level. Global heat transfer calculations performed during design phase and confirmed afterwards by Burn (1997) indicate that this flow rate exceeds the required value to keep temperatures at an acceptable level. The main objective of the experiments will be to confirm the parameters chosen for the design of the system in a more detailed configuration since it considers, for example, the spatial distribution with a mock-up in natural scale for both the core as well as the spray header.

4. The experiments

In order to validate the chosen design parameters and also to demonstrate the safety characteristics of the system to licensing authorities (to obtain the certification to upgrade the power to 5 MW), two experiments were conducted, namely: The Spray Flow Distribution Experiment and The Heated Plates Experiment.

4.1. The spray flow distribution experiment

This experiment was conducted to define the type, the quantity and the position of the spray nozzles in the distribution header positioned above reactor core. The experiment was based primarily on the measurement of the water volume received by each of the core components during a time interval. With this experiment it was possible to verify and to reduce the shadowing effect caused by the control fuel elements which are higher than the normal fuel elements obstructing the flow spraying to the later ones.

The experimental setup is composed by a test section which mocks-up in full scale, the core region of the reactor. In addition, a spray header in U form is assembled above the core which allows for different heights, number, type and positions of spray nozzles. Every core component water level is monitored through a level board. The experimental setup is illustrated in Fig. 5.

The test section is composed of 72 dummy elements arranged in a 9×8 matrix configuration, simulating in natural scale the fuel elements, control elements, reflector elements and irradiation elements. Besides the core components it also included parts of the core support structure and the in-core neutron detectors support tubes. The active core is represented in the test section by 25 fuel elements in a 5×5 array configuration being 21 normal fuel elements and four control fuel elements. The simulated fuel elements were manufactured using 3×3 in. (76.2×76.2 mm) square aluminum frames, which are the approximate fuel elements external dimensions. The relative heights of each simulated component was kept at its original value. The upper end of the simulated fuel elements are open and the lower end is closed having a connector for a transparent plastic tubing of 6 mm diameter used to monitor the water level. The simulated control fuel elements have their top end closed. The water cooled spray enters through two existing lateral rectangular windows located 5 mm below the top end. Figs. 6 and 7 show schematically the test section, the fuel elements identification in the core and the spray nozzles positions.

The spray header is a U shaped 2 in. PVC tube assembly equipped with seven spray nozzles with flexible connectors allowing for different angular directions. After running several tests using 26 different spray nozzles configurations we chose the configuration composed by six conic jet type (Full Cone Nozzle) with 0.5 in. and 45° spraying angle and one plane jet type (Flat Jet Nozzle) with 0.25 in. and 30° spraying angle. The nozzles choice was based on the total water flow rate and pressure head available as well as on the resulting flow distribution on the core for the header positioned 525 mm above the fuel elements.

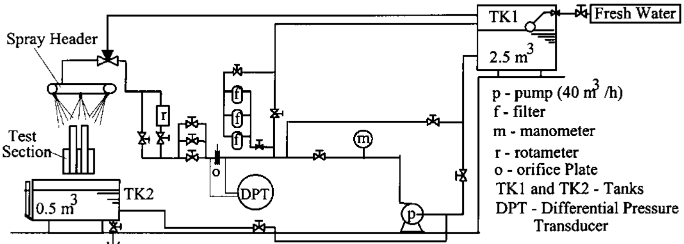

Fig. 5. Experimental setup for spray flow distribution experiment.

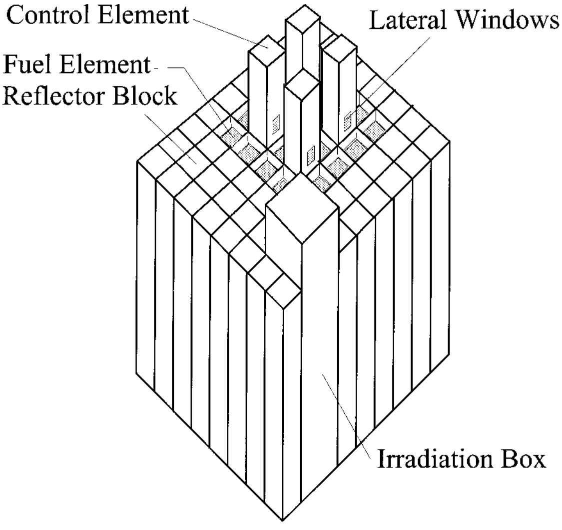

Fig. 6. Schematic drawing of test section.

In Fig. 8 the experimental results for the normalized flow rate distribution using the chosen configuration operating at three total flow rate values: 2.0, 2.5 and 3.0 m^3/h are shown. The efficiency of the distribution calculated as the ratio between the individual fuel elements flow rate to the total flow rate is around 65%. For the design flow rate all elements had flow rates over 30 $cm^3/min/plate$. The control elements which have only lateral water passages, represented by numbers 7, 9, 17 and 19, had even larger flow rates.

4.2. The heated plates experiments

The main objective of this experiment is to demonstrate the effectiveness of the spray system in cooling the fuel elements after the ocurrence of a total loss of water in the reactor pool. To perform heated plates experiment under uncovered core condition, the test section STAR shown in the Fig. 9 was designed. The heated region is simulated by four plates connected in series and electrically heated to simulate the fuel plates and the cooling channels between them. The plates ($625 \times 59 \times 1.4$ mm) are made of a 80% Ni and 20% Cr alloy with 10 type K 0.5 mm diameter ungrounded thermocouples stainless steel cladded. The thermocouples position and identification on plates 2 and 3 can be seen in Fig. 9. The plates were assembled in the center of a 3×3 in. aluminum frame with square cross section and electrically isolated with Celeron. To fully simulate a MTR type fuel geometry, 12 aluminum plates 1.58 mm thickness with no heating were also assembled at both sides of the heated plates. The electrical supply is carried out by a current rectifier with 24 kW capacity (12 VDC; 2000 A) which allows for power adjustments

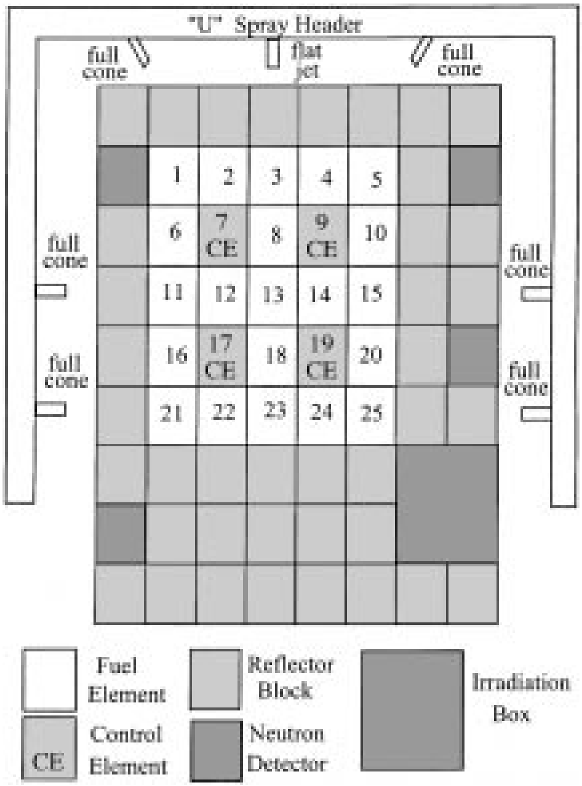

Fig. 7. Fuel element identification in the core.

in steps. A personal computer equipped with a National Instrument board and LabWindows software (National Instruments, 1995) were used for data acquisition.

The heated plates experiments were performed in the same experimental setup used for the spray flow distribution experiments. The STAR test section was installed in place of the fuel element 12 as shown in Fig. 7. This setup made it possible to simulate the heated plates in a more realistic environment, including the shadowing effects from neighbour components. The water coolant was recirculated between the tank TK2 and the pump at a constant flow rate of 3.5 m^3/h in each and every experiment.

Two types of experiments were conducted, both over a 1 h period. In the first set of experiments named STAR53 and STAR54, the heat flux imposed to the plates corresponded to the mean heat flux in the channel in the core with the maximum integrated energy and not the one with the maximum local peak heat flux. Due to the direct electrical heating of the plates no axial profile of the heat flux was obtained. It was used instead a equivalent uniform flux. This test can be considered

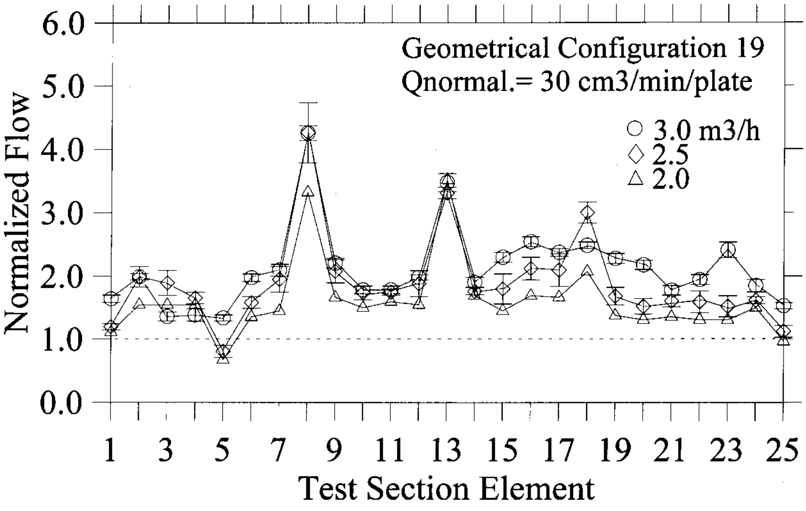

Fig. 8. Normalized flow distribution.

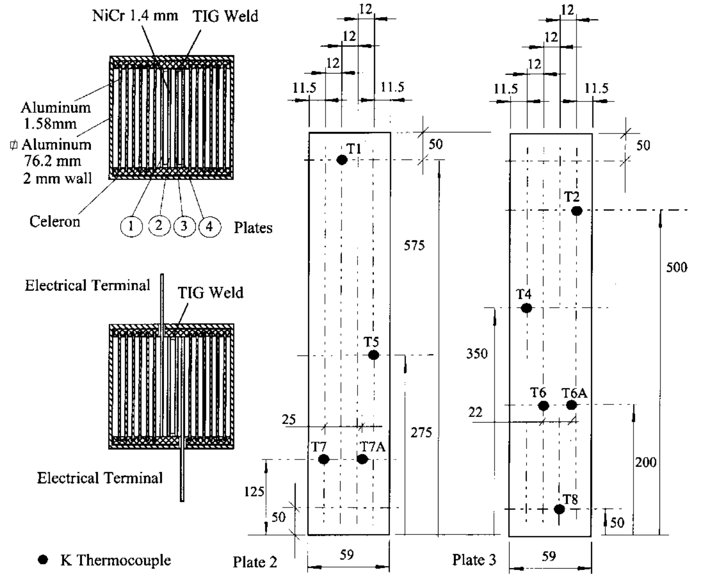

Fig. 9. STAR test section and thermocouples positioning in plates 2 and 3.

as the most conservative since it represents a fuel channel with 40% more energy than the mean core condition.

The second set of experiments named STAR55 and STAR56 simulates a hypothetical fuel channel where the heat flux is uniform and equal to the maximum peak flux in the entire core. The energy generated in this channel is 66% higher than the energy generated in the channel where the peak heat flux occurs, and 150% higher than the mean core condition.

During the experiment the rectifier power was changed in steps to follow the same behavior as the calculated decay heat curve. The duration of every experiment was 1 h, considering as the initial condition the decay heat corresponding to t=300 s (~140 kW) after shutdown, Fig. 2. Preliminary testings indicated that the critical period occurs during the first 30 min.

4.2.1. STAR53 test

Fig. 10 shows qualitatively the axial heat flux distribution in the channel with the largest energy integral and the actual uniform heat flux used in the STAR53, both with the same energy equivalence. The actual uniform heat flux time history used in the experiments is shown in Fig. 11.

The recorded temperatures by the thermocouples welded on the plates 2 and 3 are shown in Figs. 12 and 13. One can observe that the critical period occurs during the first 30 min of the transient when the temperature reaches a maximum of 330°C in the plate 2 and 230°C in plate 3 below the design limiting temperature of 500°C. During the second half of the experiment the temperatures are lower due to the reduction in the heat fluxes to follow the decay curve.

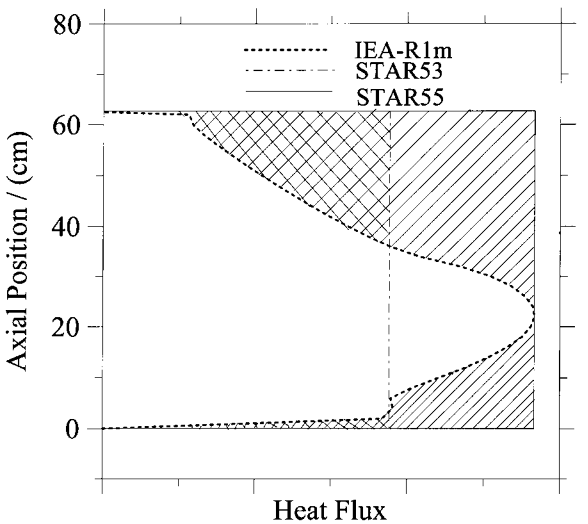

Fig. 10. Experimental and theoretical heat flux profile.

Although the thermocouples 6/6A and 7/7A are located pairwise at the same axial position but in different plates, they recorded very different temperature time history as can be noted in Figs. 12 and 13. This behavior can be explained by observing the water flow pattern in the channels. It was observed visually during the experiments that the cooling process is composed both by water evaporation as well as heat convection to flowing water. The flow pattern presents a peculiar behavior in the form of "fillets" running along the entire channel. The difference between the measured temperatures from two adjacent thermocouples is due to the particular position of this "fillet" in relation to the thermocouples position. It can be noticed that sometimes one thermocouple indicates a higher temperature than its adjacent pair and some times this relation is inverted indicating that the position of the water "fillet" is changing.

Other test was performed in order to check repeatability of the experiment (e.g. STAR54). The temperature time history showed some differences caused by the different positioning of the water "fillets" but the average and maximum conditions were repeated.

In order to explain how this peculiar cooling flow pattern can affect the resulting temperature distribution, a numerical 2D model was developed to solve the stationary conduction equation for the plate. The model also allows for comparison of the influence on temperature gradients caused by the difference between the experimental plates and the actual fuel elements material properties.

4.2.2. STAR55 test

Fig. 10 shows the axial heat flux distribution at the hot channel, i.e. the channel with the maximum heat flux value in the core, and the uniform heat flux value used

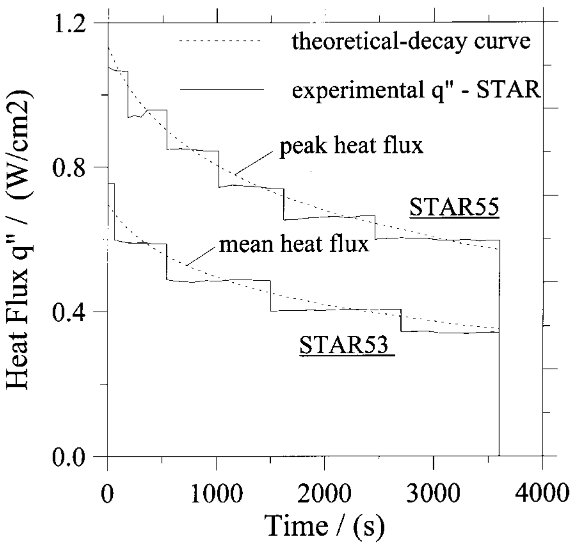

Fig. 11. Experimental and theoretical heat flux time history.

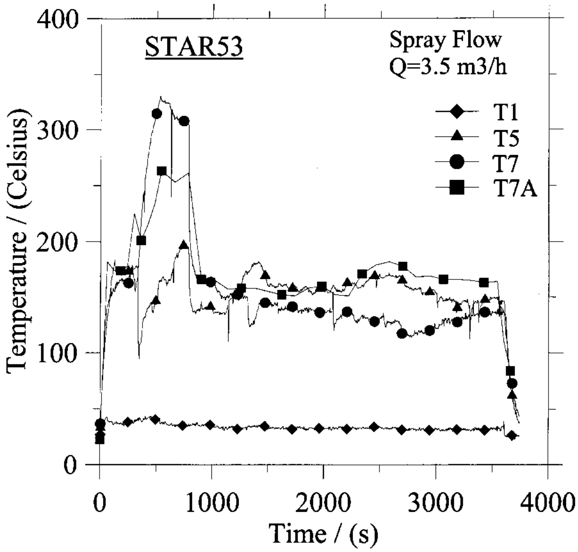

Fig. 12. Temperatures in the plate 2 – STAR53 test.

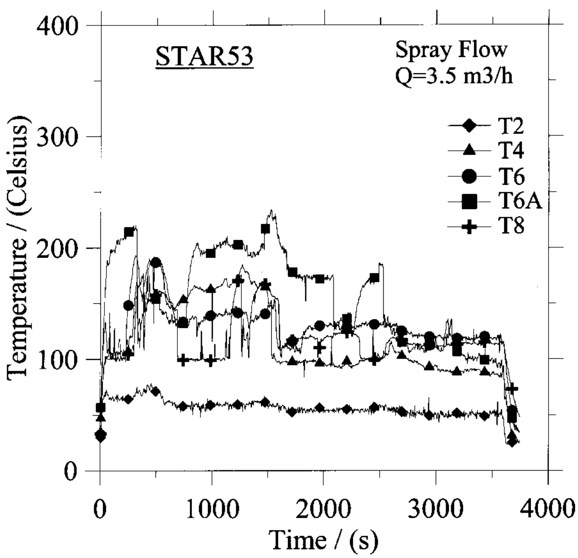

Fig. 13. Temperatures in the plate 3 – STAR53 test.

in the experiments. Fig. 11 shows the time history of the peak flux and the stepwise experimental simulation of the decay heat curve.

As mentioned before, the total energy delivered during this experiment is 66% higher than the actual energy delivered in the core, as can be seen in the shadowed area of Fig. 10. Therefore, the experimental conditions far exceed the maximum energy input possible during the accident and even though the maximum temperatures were below the limiting design value of 500°C.

The experimental measured temperatures are shown in Figs. 14 and 15. In this case it is also observed that the most critical period is the first 30 min, when the maximum observed temperatures are in the range between 330°C and 400°C, respectively in the plates 2 and 3.

In these tests, a similar behavior compared to the previous tests was observed for the adjacent thermocouples 6/6A and 7/7A as depicted in Figs. 14 and 15. It can be observed for example that at a certain instant, the temperature at the thermocouple 7A drops suddenly to 100°C staying at this value for some time. This fact can be explained by the direct cooling of a water "fillet" flowing very close or even on the thermocouple.

Another test STAR56 was conducted in similar conditions to check for repeatability, and the results compared to the STAR55 showed that, although the time history is somewhat different, the maximum temperatures were also below limiting value. The dependence of the temperatures time histories on the particular position of the water "fillet" is the cause for the difference between tests but the repetition of the maximum temperatures values demonstrate that the overall energy balance is

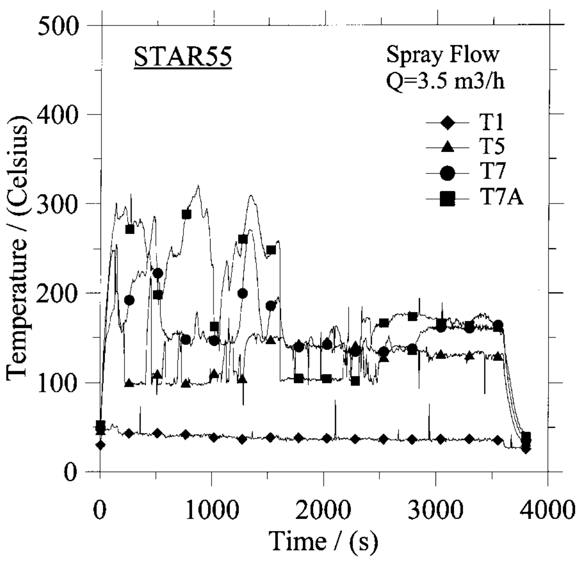

Fig. 14. Temperatures in the plate 2 – STAR55 test.

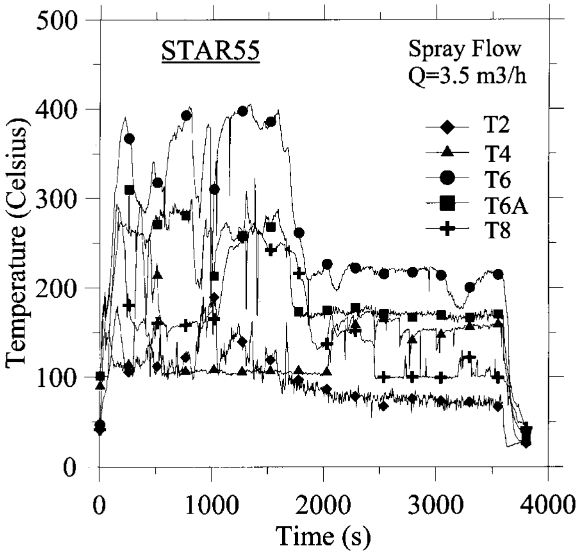

Fig. 15. Temperatures in the plate 3 – STAR55 test.

kept and enough to assure that no limiting temperature values will be violated. This will be further analysed below by modelling where the water "fillet" will be positioned in the most conservative condition.

5. Heat conduction modelling

The differences in the results observed between tests performed under identical conditions and the difference in the temperature time history during the same experiment measured by adjacent thermocouples lead us to further investigate the heat transfer regime in the plates. In the first phase of the investigation, visual observation of the plates indicated that the flow pattern formed during the plates cooling has the form of "fillets" and the water evaporation with mineral salts crystallization leave a footprint on the plates allowing visual observation of the flow pattern as illustrated in Fig. 16.

Comparison between the results obtained in different tests showed that the flow pattern on the heated plates are not repeated, following different trajectories for each test. This behavior, i.e., changes in the position of the water "fillets" relative to the thermocouples, is responsible for the different temperature time history measured in each identical test. Due to this peculiar flow pattern behavior and also due to the impossibility of installing more thermocouples to give higher resolution in the experimental mapping of the temperature time history, a numerical model is necessary to complement the experimental data in order to reach a safe conclusion.

In order to verify the effect of different possible positions of the "fillets" upon the maximum temperatures and also to extrapolate the results from the experiments where the heated plate material is a Ni–Cr alloy to that of the fuel elements where the material is an Al–UO_2 alloy, a 2D heat conduction model Eq. (1) was developed using finite difference techniques.

$$\rho c\frac{\partial T}{\partial t}=q''' + k\left(\frac{\partial^2 T}{\partial x^2}+\frac{\partial^2 T}{\partial y^2}\right), \tag{1}$$

where ρ is the material density in kg/m^3, c is the material specific heat in J/kg. °C, q''' is the volumetric thermal source in the plate in W/m^3, k is the material thermal conductivity in W/m. °C and T is the temperature in °C.

The spatial domain discretization is shown in Fig. 17 with the plate width divided into ii = 30 nodes and the thickness into jj = 5 nodes. The heat transfer coefficient for the water "fillets" was calculated using Thom's correlation (Thom et al. (1965)), given by Eq. (2), and for natural convection cooling by air, a constant value of 7.5 W/m^2 °C was used.

$$T_{\mathrm{w}} - T_{\mathrm{sat}} = 22.65\phi^{0.5}\,\mathrm{e}^{-P/87}, \tag{2}$$

where T_{w} and T_{sat} are the plate surface and saturation temperatures in °C, ϕ is the heat flux in MW/m^2 and P is the absolute pressure in Bar.

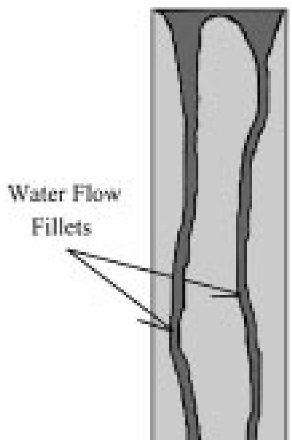

Fig. 16. Pictorial side view of a plate showing "fillets" flow pattern.

The measured experimental volumetric flow rate for each individual channel was always larger than 45 cm^3/min/channel, which is sufficient to cool the entire channel even for the most critical condition when the core maximum heat flux value of 1.133 W/cm^2 is used. Under this condition, an overall energy balance showed that the fraction of water evaporated is around 30% from the entrance of the channel down to the bottom. This fact indicates that a constant "fillet" width and thickness model will not introduce significant errors in the solution.

Fig. 18 shows the steady-state surface temperature results from the numeric model where only one 4 mm width water "fillet" was considered at 22 mm from the heated plate border and 600 W power which is equivalent to a heat flux of 0.8 W/cm^2. Two solutions are shown: one using the thermal conductibility of the experimental heated plate material (Ni–Cr) which is 12 W/m°C and another using the thermal conductibility of the fuel elements (AL–UO_2) which is 144 W/m°C. The smaller value of the thermal conductibility used in the experiments causes a correspondent difference in temperature gradients between the experimental heated plates and the actual fuel element. When in the experiments the maximum temperatures were above 250°C, under identical conditions, the actual fuel elements maximum temperatures should be around 150°C.

One can also notice that when in the Ni–Cr plate thermocouple T7 measures 150°C and its adjacent thermocouple T7A registers 200°C, the correspondent temperatures in the actual fuel element would be 120°C and 140°C, respectively. A similar behavior is observed at the T6 and T6A thermocouples positions. These numerical results explain the data obtained during the STAR53 and STAR55

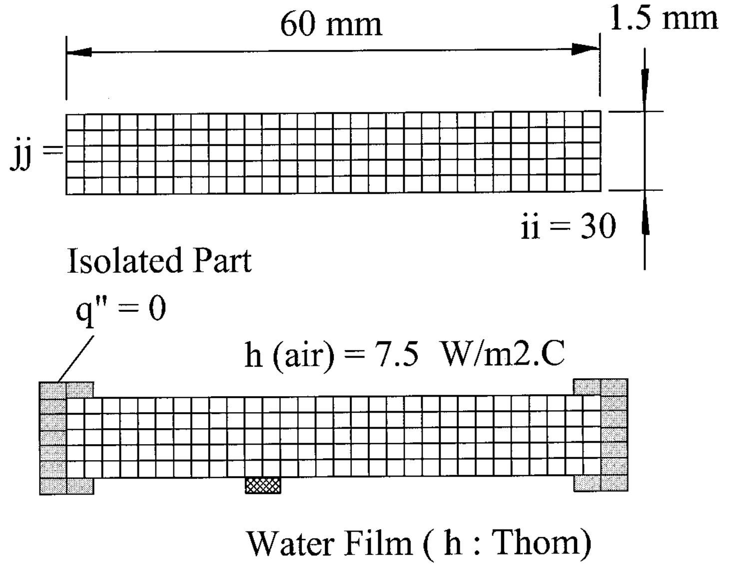

Fig. 17. Heated plate cross section – 2D discretization.

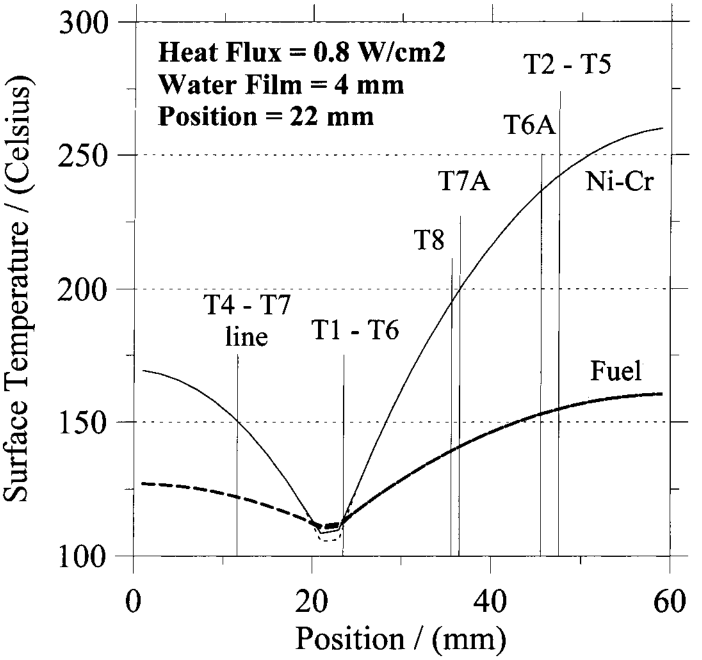

Fig. 18. Temperature distribution – q'' =0.8 W/cm^2.

experiments and offer a phenomenological insight for the temperature difference measured at two adjacent position.

Fig. 19 analyses the effect of more than one water "fillets" and of their widths. Two "fillets" with 2 mm width each positioned at 27 and 51 mm from the border were simulated, keeping the heat flux at 1.103 W/cm^2. Under these conditions the maximum calculated temperatures for the Ni–Cr heated plates were around 500°C and the correspondent maximum temperature in the fuel is 150°C. Figs. 18 and 19 indicate the position of the installed thermocouples so that they can be used to interpret the experimental data and to extrapolate for the actual core condition.

6. Conclusions

The design of the emergency core cooling system of the IEA-R1m research reactor, upgraded to operate at 5 MW, used conservative parameters and redundancy criteria to assure that, in the ocurrence of the postulated total loss of pool water, the maximum fuel temperatures will be kept at safe levels. The spray flow distribution experiments defined the spray header specifications and demonstrated that every core component including the control elements are adequately irrigated by the spray

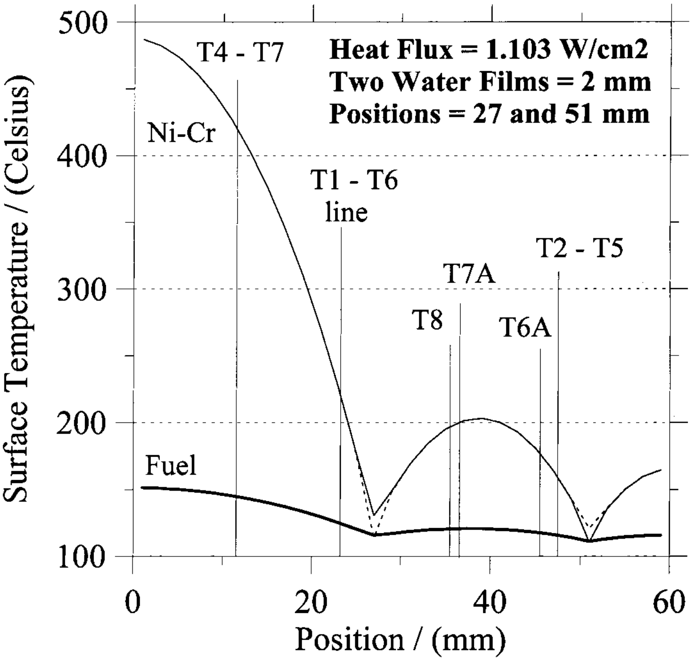

Fig. 19. Temperature distribution – $q'' = 1.103$ W/cm^2.

system. The heated plates experiments demonstrated that during the first 30 min critical period, even under very conservative conditions, the maximum temperatures were well below the 500°C limit. The numerical modelling is able to demonstrate and to explain the peculiar water "fillets" flow pattern and cooling regime and also to calculate the actual fuel elements temperatures which are quite smaller than the temperatures measured experimentally due to different thermal conductibility.

References

Burn, R.R., 1997. Final report technical cooperation test – IPEN – IEA-R1m Research Reactor RLA/0/016-45 Nuclear Technology Support, Internal Report

Croff, A.G., 1980. ORIGEN-2, Isotope Generation and Depletion Code, ORNL-TM-7175, Oak Ridge National Laboratory

Flowler, T.B., Vondy, D.R., Cunnigham, G.W., 1971. Nuclear Reactor Core Analisys Code: CITATION, ORNL-TM-2496 Ver. 2, Oak Ridge National Laboratory

Gehre, G., Hieronymus, W., Kampf, T., Ringel, V., Roßbander, W., 1989. The modification of Rossendorf research reactor – technical performance and responsibility of control and licence authorities, Proceedings of International Symposium on Research Reactor Safety Operations and Modifications, vol. 3, Ontario, Canada, p. 849

Kerr, W., King, J.S., Martin, J.C., Wehe, D.K., 1991. The nuclear ford reactor demonstration project goes the evaluation and analysis of low enrichment fuel – Final Report – Argonne National Laboratory, Argonne, ANL/RERTR/TM-17

Maprelian, E., 1997. Programms LOSS and TEMPLOCA for accidents analysis of loss of coolant in the IEA-R1m – IPEN Report no. PSI.RAS.IPEN.004-RELT.001.R00

National Instruments, 1995. LabWindows/CVI – Visual Programming For Instrumentation – Programmer Reference Manual, 1995

Parkanski, D., 1992. Sistema de refrigeracion por rociado de um reactor tipo piscina, Proceedings of IV-CGEN - General Congress of Nuclear Energy, vol. 1, Rio de Janeiro, p. 125

Thom, J.R.S., Walker, W.M., Fallon, T.A., Reising, G.F.S., 1965. Boiling in subcooled water during flow up heated tubes or annuli, Proceedings of Inst. Mechanical Engineering, Part 3c, p. 180

Webster, C.C., 1967. Water-loss tests in water-cooled and -Moderated Research Reactors. Nuclear Safety 8(6), 590.

Williams, H.T., Stopinski, O.W., Yarnell, J.L., Lyle, A.R.,Warner, C.L., Maine, H.L., 1969. Status Report on Omega West Reactor, with Revised Safety Analysis, LA-4192.30